Rapid magnetic resonance elastography of skeletal muscle using one dimensional projection.

S.F. Bensamoun, K.J. Glaser, S.I. Ringleb, Q. Chen, R.L. Ehman, K.N. An

Original Research

Rapid Magnetic Resonance Elastography of Muscle Using One-Dimensional Projection

Sabine F. Bensamoun, PhD,[1] Kevin J. Glaser, PhD,[2] Stacie I. Ringleb, PhD,[1] Qingshan Chen, MS,[1] Richard L. Ehman, MD,[2] and Kai-Nan An, PhD[1]*

Purpose: To demonstrate the feasibility of 1D MR elastography (MRE) to rapidly assess skeletal muscle stiffness in vivo.

Materials and Methods: Shear waves were induced in the vastus medialis muscle (VM) using a pneumatic driver at 90 Hz and 2D MRE data were collected. Spatially selective excitations were used to produce 1D projections of MRE data oriented along the direction of propagating waves in the muscle. Data were collected with the thigh muscles relaxed and contracted at 20% maximum voluntary contraction (MVC) and the knee flexed at 30°.

Results: The muscle stiffness measured at rest and in contraction with 1D MRE was 3.69 ± 0.80 kPa and 9.52 ± 2.74 kPa, respectively, and 4.36 ± 0.98 kPa and 9.22 ± 1.29 kPa, respectively, with the 2D MRE technique.

Conclusion: Muscle stiffness measured using 1D MRE was in agreement with 2D MRE while reducing the scan time by a factor of 4.

Key Words: 2D magnetic resonance elastography; 1D beam elastography; thigh muscle; elastic properties
J. Magn. Reson. Imaging 2008;27:1083–1088.

SKELETAL MUSCLE is composed of contractile (myosin) and elastic passive (actin, connective tissue) components (1). These elements interact to generate and to transmit force through the tendon. Invasive biopsy (2) and electromyography (EMG) with needle techniques (3,4) as well as noninvasive techniques using palpation, ultrasound (5–7), and MRI (8,9) have been investigated to quantify the structural (muscle volume, cross sectional area, pennation angle) and functional (mitochondrial function, glycolytic function, contractile efficiency) parameters of skeletal muscle. To completely characterize muscle disease it is necessary to understand the changes that occur at the structural, functional, and cellular levels.

In the past three decades magnetic resonance imaging (MRI) and spectroscopy have been developed to visualize and characterize internal structures including organs and skeletal muscle (10). In the past decade MR elastography (MRE) (11) was developed to quantify and to image the spatial distribution of the in vivo mechanical properties of soft tissue, such as muscle elasticity (12–14). MRE is a novel noninvasive phase-contrast MR technique capable of visualizing small amplitude wave propagation (on the order of microns) from externally applied shear motion (11). The measured waves can be used to produce an image, or elastogram, of the spatial variations of stiffness throughout the tissue.

In a previous study (15) it was shown that 2D MRE was capable of measuring the stiffness of relaxed and actively contracted thigh muscles, and it was determined that there was a significantly different stiffness in the vastus medialis (VM) when contracted compared to the relaxed state. That 2D MRE acquisition included a 256 × 64 acquisition matrix, four time offsets, two polarities of the motion-encoding gradient, and TR = 350 msec, which yields an acquisition time of 3 minutes. While an MRE acquisition time of 1–3 minutes may be satisfactory for imaging skeletal muscle in the relaxed state, it is not desirable for studying the muscle under active loading at any significant fraction of maximum voluntary contraction (MVC) because the muscle will fatigue.

The acquisition time for MRI and MRE can be reduced by reducing the TR and reducing the number of phase encodes that have to be performed. In a previous study (16) it was shown that MRE acquisition times could be reduced by a factor of 8 using reduced-FOV (field of view) imaging techniques, and by a factor of 64 using 1D projection techniques, while still producing stiffness estimates comparable to conventional 2D MRE. That work demonstrated in a phantom study that MRE data could be acquired using 1D imaging in just a few seconds.

The purpose of this study was to assess the potential of 1D MRE for skeletal muscle imaging by measuring

[1]Biomechanics Laboratory, Division of Orthopedic Research, Mayo Clinic College of Medicine, Rochester, Minnesota.
[2]Department of Radiology, Mayo Clinic College of Medicine, Rochester, Minnesota.
Contract grant sponsor: National Institutes of Health (NIH); Contract grant numbers: EB00812, EB001981, CA91959, HD07447.
*Address reprint requests to: K.-N.A., PhD, Biomechanics Laboratory, Division or Orthopedic Research, Mayo Clinic College of Medicine, 200 First St., SW, Rochester, MN 55905. E-mail: an.kainan@mayo.edu
Received May 10, 2007; Accepted January 3, 2008.
DOI 10.1002/jmri.21307
Published online 11 April 2008 in Wiley InterScience (www.interscience.wiley.com).

the stiffness of the vastus medialis (VM) in the relaxed and contracted states and comparing those stiffness estimates to those from conventional 2D MRE.

MATERIALS AND METHODS

Participants

Six volunteers (males, age 26.6 ± 3.8, range 23–32, body mass index [BMI] 23.30 ± 2.27) participated in this MRE study. The study was approved by the Institutional Review Board and written informed consent was obtained.

Experimental Setup

The experimental setup was designed similar to a previous study (15). The volunteers lay supine in a 1.5T General Electric Signa (Milwaukee, WI) MRI machine. The right leg was placed in a positioning device. An adjustable device maintained the shoulders in a fixed position and the right knee was positioned in 30° of flexion. The right foot was placed on a footplate and secured with a Velcro strap. The footplate was composed of two MR compatible loads cells (Interface, Scottsdale, AZ): one to measure the horizontal force and the other to measure the vertical force. A custom-made Labview (National Instruments, Austin, TX) program recorded the forces and gave the volunteer visual feedback to ensure the desired force was maintained. The MRE tests were conducted in the relaxed position (no contraction) and 20% of maximum voluntary contraction (MVC).

External vibrations were applied to the thigh muscles with a pneumatic driver positioned on the thigh 1/3 of the distance from the patellar tendon to the greater trochanter. Only the shear (or transverse) waves produced by these vibrations are tracked and measured inside the muscle due to their small wavelengths compared to the much higher wave speed and wavelength of the accompanying longitudinal waves. The pneumatic driver consisted of a remote pressure driver (ie, a large active loudspeaker) connected by a long hose to a smaller silicone tube wrapped around the subject's thigh. This system created a time-varying pressure wave, which caused the tube around the thigh to expand and contract with the remote driver at 90 Hz. A custom-made Helmholtz surface receive coil was placed around the thigh for data acquisition.

2D MRE

2D gradient echo (GRE) MRE was used to obtain oblique images of the thigh muscle as in the previous study (15) and briefly summarized here. The MRE pulse sequence included a motion-encoding gradient which oscillated at the same frequency as the driver (90 Hz) and was used to image the through-plane component of displacement of the shear waves. The imaging plane was oriented along the VM muscle and MRE images were collected at four time offsets (phase offsets) between the start of the motion and the motion-encoding gradients that were evenly spaced over one period of the motion to image the wave propagation over time. The acquisition matrix was 256 × 64, which was interpolated to 256 × 256, and the flip angle was 45°. The TR was 275 msec and the TE corresponded to the minimum echo time that allowed for motion encoding (≈19 msec). This resulted in an acquisition time of 141 seconds.

2D MRE Image Processing and Data Analysis

The processing and analysis of the 2D MRE data were the same as in a previous study (15) and are briefly summarized here. Line profiles were drawn along the VM (Fig. 1) and the shear wavelength manually estimated in each of the four phase offsets and the average value was calculated. Assuming a simple elastic model for the muscle, the shear stiffness was estimated as $\mu = \rho(f*\lambda)^2$, where μ is the shear stiffness, ρ is the density of the tissue (assumed to be 1000 kg/m^3), f is the frequency of the motion, and λ is the shear wavelength.

1D Beam MRE

1D beam MRE, also previously described (17), was performed during the same exam on each volunteer using a modified version of the above 2D GRE MRE sequence. The slice-selective RF pulse was replaced with a 2D spatially selective RF pulse (18) to excite a column of spins, and the phase encoding gradient waveforms were turned off to measure the excited region as a 1D profile. The *k*-space trajectory for the selective excitation was designed using a variable-density spiral algorithm (19) to create a constant-density, center-seeking spiral trajectory that was discretely evaluated using the technique developed by Hardy and Cline (20). The algorithm allows for a smooth transition between the gradient slew-rate limited region of the trajectory at the center of *k*-space and the gradient amplitude limited region at the edge of *k*-space. The RF waveform was calculated to excite a cylindrical column of spins with a 2D circular Gaussian cross-sectional profile with the beam width defined to be six standard deviations of the Gaussian profile. The selective excitation waveforms were 20 msec long calculated using a 24 cm excitation FOV, 2.2 G/cm maximum gradient amplitude limit, 11.9 G/cm/ms maximum gradient slew-rate limit, and a desired 12 mm diameter spatial excitation. Fat chemical presaturation was performed on each TR to reduce the effects of the off-resonant fat signal in the beam MRE profiles.

The imaging parameters for the 1D MRE acquisition were similar to those for the 2D MRE acquisition above: 256 frequency encodes, 16 Nex, 45° flip angle, 275 msec TR, TE ≃ 19 msec, four time offsets evenly spaced over one period of the 90 Hz motion. The acquisition time for the 1D MRE data was therefore one-fourth of that for the 2D MRE data, or about 35 seconds.

The 1D MRE imaging sequence also has the capability of showing the location of the beam with respect to the anatomy by using the spatially selective excitation as a spatial presaturation pulse in a 2D GRE acquisition. Each of these localization acquisitions was equivalent to a single phase offset 2D MRE acquisition with no externally applied motion, so each took about 35

seconds for this study. The center of the beam was placed in the VM near the location of the MRE driver and rotated until the beam was oriented in the direction of the VM, which was typically 60° from horizontal in these oblique images (Fig. 2a). It was assumed that the most accurate wave information would be obtained in this orientation because, based on the 2D MRE data from the previous study of the VM (15), this is the approximate direction of wave propagation in the VM. It typically took only a couple of these localization scans to verify the location and orientation of the beam in the VM and thus only added a couple of minutes to the total exam time. To demonstrate the sensitivity of the 1D MRE technique to alignment with the wave propagation direction in the VM, MRE data were collected with the beam rotated to several other orientations as well (Fig. 2d).

1D Beam Image Processing and Data Analysis

The Fourier transform through time was calculated for each dataset and the first harmonic (90 Hz) of the Fourier transform was taken for further analysis. For a single shear wave the real and imaginary parts of the first harmonic of the Fourier transform will have spatial oscillations with a wavelength equal to that of the shear wave. The shear wavelength in the VM was estimated manually from the real and the imaginary parts of the first harmonic of the 1D MRE data (Fig. 2c) and the two estimates were averaged together. Like for the 2D MRE data, the shear wavelength measured using the 1D MRE data was then used to estimate the shear stiffness.

Statistical Analysis

T-tests were performed with the software Statgraphics 5.0 (Sigma Plus, College Park, MD) in order to compare the VM stiffness measured with the 2D MRE and the 1D beam MRE techniques ($P < 0.05$).

RESULTS

Figure 1 shows an example of shear waves propagating inside the belly of the VM muscle using 2D MRE while the muscle was relaxed. The phase image (Fig. 1b) shows the amplitude variation of the shear waves. A profile was drawn along the wave propagation direction to measure the wavelength when the muscle was relaxed and contracted. The propagation of the shear waves was consistently observed in these oblique imaging planes inside the VM corresponding to an orientation of 60°.

Figure 2a shows the VM muscle with the beam oriented at 60° and located in the same anatomic area as the previous profile used for the 2D MRE analysis. The visualization of the shear waves propagating inside the VM muscle was clearly observed during the four time offsets and is represented by the successive red (peak of the wave) and blue (trough of the wave) bands (Fig. 2b). Figure 2c shows the real part of the first temporal harmonic of the phase data from Fig. 2b. The shear waves were consistently observed when the direction of the beam was oriented at 60° within the muscle in both the relaxed and contracted state. The shear wave profiles obtained with the 2D MRE (Fig. 1c) and 1D beam MRE (Fig. 2c) techniques are very similar.

Figure 2d–f shows an example of the 1D MRE acquisition when the beam excitation for the 1D MRE acquisition was not oriented at 60°. The magnitude image in Fig. 2d shows that the beam is oriented transversely to the VM. The individual phase offsets (Fig. 2e) as well as the real part of the first harmonic (Fig. 2f) show no clear depiction of the shear wave. It is not possible to measure the wavelength of the shear waves in these conditions.

The mean stiffness of the VM for all six volunteers measured in the relaxed position with the 2D MRE and 1D beam MRE techniques was 4.36 ± 0.98 kPa and 3.69 ± 0.80 kPa, respectively. During a contraction of 20% MVC the shear modulus of the VM measured with the 2D MRE and 1D beam MRE techniques was 9.22 ± 1.29 kPa and 9.52 ± 2.74 kPa, respectively. The result of the statistical analysis showed no significant difference of muscle stiffness between the 2D MRE and 1D beam MRE techniques in either the relaxed or the contracted states ($P < 0.05$).

The frame rate for the 1D MRE technique can be increased by reducing the number of averages performed. This allows for a more real-time assessment of changes in the muscle stiffness. Figure 3 shows a 1-Nex 1D MRE acquisition in the VM in which the volunteer was asked to hold 10% MVC for 15 seconds, and then progressively increase the exertion in 10% MVC steps up to 50% MVC, holding each step for 15 seconds. The horizontal axis represents spatial position along the beam, while the vertical axis is time-sampled in 400-

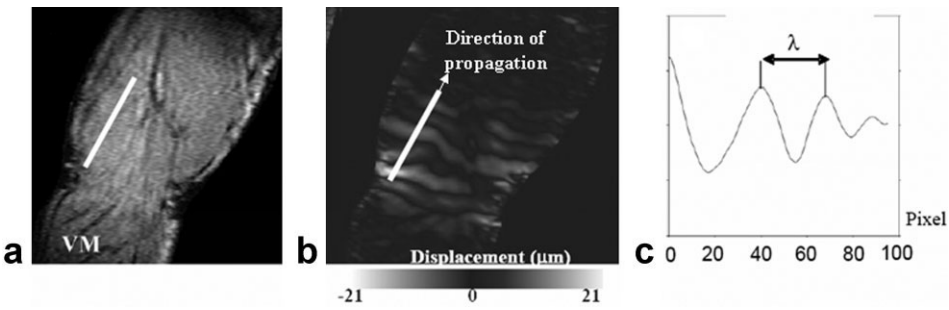

Figure 1. a: MR image of the oblique plane prescribed in the vastus medialis (VM) muscle. **b:** Phase image indicating wave displacement with the white profile drawn along the direction of wave propagation. **c:** Phase data along the indicated profile in (b) indicating the wave traveling along the profile.

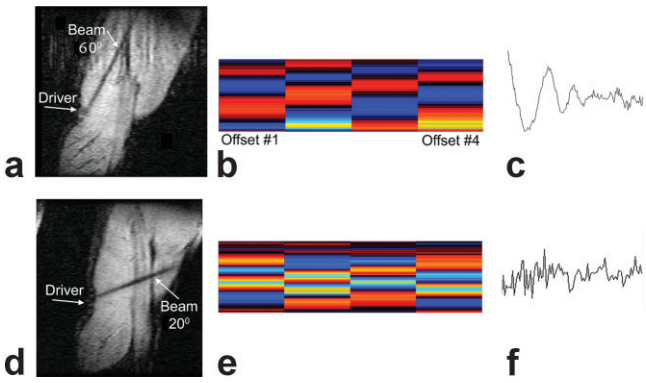

Figure 2. a,d: MRI picture of the oblique plane prescribed in the vastus medialis (VM) muscle with the beam oriented at (a) 60° and (d) 20°. **b,e:** Phase data at the four time offsets (horizontal axis) along the beam indicating the shear wave propagation along the beam (vertical axis). **c,f:** Image of the real part of the first harmonic of the wave along the beam. A wave is clearly visible in (c), while (f) shows that there was no measurable wave with a beam orientation of 20°.

msec increments (or 2*TR, where the TR for this acquisition was 200 msec). The results indicate an increase in the shear wavelength, and thus the shear stiffness, as the exertion level increases.

DISCUSSION

The purpose of this study was to demonstrate the feasibility of 1D MRE to rapidly assess skeletal muscle stiffness while providing stiffness estimates comparable to 2D MRE. While the determination of the thigh muscle (vastus lateralis, vastus medialis, sartorius) stiffness using 2D MRE was previously shown (15), the disadvantage of this 2D MRE technique was the time of acquisition, which was typically several minutes depending on the TR, the number of phase encodes, and the number of phase offsets. The continuity of this work was to find a faster method to measure the thigh muscle stiffness in order to reduce muscle fatigue during the MRE exam.

The use of spatially selective excitations can significantly reduce scan times in MRI. In a previous study it was demonstrated in gel phantom experiments that MRE displacement information measured along 1D projections (beams) could be used to estimate the shear stiffness distribution along the length of the beam (16). Additionally, it was shown that the stiffnesses measured through stiffer and softer agarose inclusions with the 1D MRE and 2D MRE sequences were similar (16). The 1D MRE technique has also been used to observe nonlinear shear wave propagation and consequently to determine nonlinear tissue properties (21). It has also been demonstrated that 1D MRE for spin echo applications using orthogonal 90° and 180° slice-selective pulses is also feasible (16). That technique was applied to imaging postmortem breast tissue with a stiff lesion. The stiffness of the breast lesion and breast tissue estimated with 1D MRE was comparable to the elastic properties measured with the 2D MRE technique.

To our knowledge the 1D MRE technique has only been applied to phantom materials and in vitro tissue to date. This study is the first to use 2D spatially selective excitations for in vivo measurements of the mechanical properties of skeletal muscle. The previous 1D MRE results (16) demonstrated a high correlation between the displacement measurements obtained with 1D MRE and those obtained using 2D MRE (correlation coefficients greater than 0.98), thus resulting in comparable stiffness estimates between the two techniques. The work presented here demonstrates the results in the more complicated scenario of imaging a dynamic, moving, viscoelastically anisotropic material. This produces several challenges that will be investigated in future work that arise because of the loss of the second imaging dimension in 1D MRE. If there is any significant variation in the stiffness of the muscle throughout its volume, then it would be important that both 2D and 1D MRE assess the same physical location in the muscle. The current experiment uses a previously documented jig to hold the leg in the correct position during the scan. However, minor changes and adjustments to the position and orientation of the volunteer are possible, especially after repetitive exertion. Future modifications to the jig may further reduce this motion and increase the quality of the registration between the 2D and 1D MRE results.

A previous study had shown that the waves propagate in an oblique direction inside the VM (unipened muscle), while inside the sartorius (longitudinal muscle) the waves follow a longitudinal direction (15). The shear waves were clearly visualized in this study with a beam oriented at 60° within the VM, which corresponds to the unipenated muscle structure. The analysis from that previous study indicated the dependence of MRE motion sensitivity and wave visibility to the alignment of the imaging plane, which motivated prescribing the 1D beam preferentially along the muscle fiber direction.

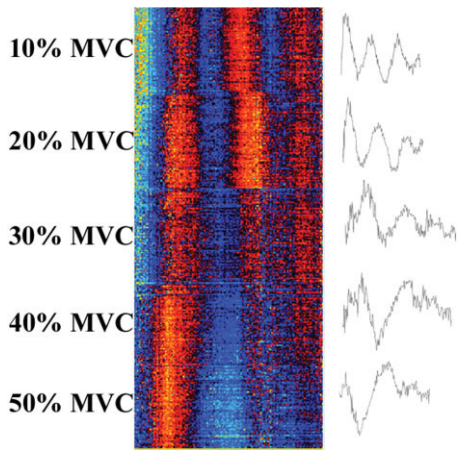

Figure 3. Real-time acquisition during different levels of contraction (from 10% MVC to 50% MVC). For each level of contraction the shear wave displacement along the length of the beam is indicated by the alternating red and blue bands in the phase data. The mean displacement at each level of contraction is shown in the profiles on the right. It is apparent that the wavelength is increasing with increasing contraction level.

In both the 1D and 2D cases the goal was to consistently target the belly of the muscle. During contraction the structure, location, and orientation of the VM may change. Effects due to changes in the location of the muscle were reduced by performing the 1D MRE localizer acquisitions while the leg was contracted. Changes in the pennation angle, geometry, and anisotropy of the muscle during contraction may produce complicated changes in shear wave speed and direction in the contracted muscle. Since the beam MRE technique does not have a second spatial dimension to help determine the propagation of the wave field, the beam MRE technique can be biased if the wave propagation is not along the axis of the beam. Since the previous 2D analysis indicated that the wave propagation direction was consistently about 60°, that orientation was fixed in this protocol. Future research will explore the degree to which these changes take place at different MVC levels and design more optimal algorithms for placing the beam in contracted muscle and processing the 1D displacement data to account for these effects.

The stiffness found for the relaxed VM with the 2D MRE (4.36 ± 0.98 kPa) and 1D MRE (3.69 ± 0.80 kPa) are within one standard deviation of each other and agree with previous estimates of the stiffness of the VM (15). At 20% of MVC the stiffness of the VM increased significantly and the measured values using 1D MRE (9.52 ± 2.74 kPa) and 2D MRE (9.22 ± 1.29 kPa) agreed well with each other. The standard deviation measured comes from the muscle biological difference is a result of the anatomic variation among the six volunteers.

The more real-time 1D MRE acquisition demonstrated in Fig. 3 may allow for the assessment of stiffness over a range of passive and active muscle contraction levels in one acquisition, including increasing and decreasing the load repeatedly to study hysteresis effects in the muscle. Future work will extend the capabilities of the acquisition to optimize and synchronize the data collection based on the exercise protocol used. Figure 3 indicates an apparent change in the SNR during the course of the experiment at different MVC levels. This loss of SNR could be due to changes in the intrinsic structure of the muscle (pennation angle) which significantly varies after 20% MVC or may indicate a change in the coupling of the motion source and transmission of the motion itself into the muscle, thus changing the wave amplitude in the muscle at different MVC levels. A decrease in the physical wave amplitude results in a decrease in the signal in the wave images (ie, the MR phase information). Therefore, while the MR magnitude signal may remain constant, thus keeping the phase error constant, the ratio between the measured wave amplitude and the phase error will decrease if the physical amplitude of motion decreases. This will yield an apparent decrease in the SNR of the wave data, which may be occurring in Fig. 3. Methods to address the changes in the muscle structure during 1D imaging will be investigated in future studies.

The 1D MRE technique demonstrated in this work has some analogy with various ultrasound elastography techniques. Techniques like sonoelastography and transient elastography can obtain stiffness information like that obtained in this work in less time using either correlation or Doppler techniques to track shear wave motion. However, MRI still has some advantages over the equivalent ultrasound techniques that may prove useful in future work. Since MRI is capable of prescribing its FOV, and thus the beam in this case, in arbitrary orientations, it may be less restricted in certain applications that have reduced acoustic windows that would affect ultrasound. Similarly, MRI provides a flexible prescription of the motion-encoding direction for MRE, even during the exam, which could prove useful in future studies of wave propagation or polarization effects down the muscle fibers. Coupling an MR-based elasticity exam, like 1D MRE, with a coregistered MR exam that obtains additional information such as fat-water content, spectroscopic information, muscle volumes and cross-sections, muscle fiber directions, etc, may increase the diagnostic power of the exam and capitalize on information that would not be obtainable with ultrasound alone and may not be as useful if the ultrasound information is not collected at the same time as the MR information.

In conclusion, this study showed that 1D MRE is able to measure shear wave displacements and stiffness inside in vivo thigh muscle. The scan time was reduced by a factor 4 (to 35 seconds with 1D MRE from 141 seconds with 2D MRE), with 1D MRE improving subject compliance during the exam. This shorter scan time would be useful for future clinical research and diagnosis, including the ability to study more muscles under more loading conditions in one exam than would currently be possible. This will allow us to improve our understanding of the effects of disease on skeletal muscle and to improve diagnosis.

REFERENCES

1. Shorten MR. Muscle elasticity and human performance. Med Sport Sci 1987;25:1–18.
2. Willan PL, Ransome JA, Mahon M. Variability in human quadriceps muscles: quantitative study and review of clinical literature. Clin Anat 2002;15:116–128.
3. Pincivero DM, Campy RM, Salfetnikov Y, Bright A, Coelho AJ. Influence of contraction intensity, muscle, and gender on median frequency of the quadriceps femoris. J Appl Physiol 2001;90:804–810.
4. Bilodeau M, Schindler-Ivens S, Williams DM, Chandran R, Sharma SS. EMG frequency content changes with increasing force and during fatigue in the quadriceps femoris muscle of men and women. J Electromyogr Kinesiol 2003;13:83–92.
5. Levinson SF, Shinagawa M, Sato T. Sonoelastic determination of human skeletal muscle elasticity. J Biomech 1995;28:1145–1154.
6. Gennisson JL, Catheline S, Chaffai S, Fink M. Transient elastography in anisotropic medium: application to the measurement of slow and fast shear wave speeds in muscles. J Acoust Soc Am 2003;114:536–5341.
7. Gennisson JL, Cornu C, Catheline S, Fink M, Portero P. Human muscle hardness assessment during incremental isometric contraction using transient elastography. J Biomech 2005;38:1543–1550.
8. Stevens JE, Walter GA, Okereke E, et al. Muscle adaptations with immobilization and rehabilitation after ankle fracture. Med Sci Sports Exerc 2004;36:1695–1701.
9. Drost MR, Heemskerk AM, Strijkers GJ, Dekkers EC, van Kranenburg G, Nicolay K. An MR-compatible device for the in situ assessment of isometric contractile performance of mouse hind-limb ankle flexors. Pflugers Arch 2003;447:371–375.
10. Griffiths Foley JM, Jayaraman RC, Prior BM, Pivarnik JM, Meyer RA. MR measurements of muscle damage and adaptation after eccentric exercise. J Appl Physiol 1999;87:2311–2318.

11. Muthupillai R, Lomas DJ, Rossman PJ, Greenleaf JF, Manduca A, Ehman RL. Magnetic resonance elastography by direct visualization of propagating acoustic strain waves. Science 1995;269:1854–1857.
12. Dresner MA, Rose GH, Rossman PJ, Muthupillai R, Manduca A, Ehman RL. Magnetic resonance elastography of skeletal muscle. J Magn Reson Imaging 2001;13:269–276.
13. Sack I, Bernarding J, Braun J. Analysis of wave patterns in MR elastography of skeletal muscle using coupled harmonic oscillator simulations. Magn Reson Imaging 2002;20:95–104.
14. Jenkyn TR, Ehman RL, An KN. Noninvasive muscle tension measurement using the novel technique of magnetic resonance elastography (MRE). J Biomech 2003;36:1917–1921.
15. Bensamoun S, Ringleb S, Littrell L, et al. Determination of thigh muscle stiffness using magnetic resonance elastography. J Magn Reson Imaging 2006;23:242–247.
16. Glaser KJ, Felmlee JP, Ehman RL. Rapid MR elastography using selective excitations. Magn Reson Med 2006;55:1381–138917.
17. Glaser KJ, Felmlee JP, Ehman RL. Rapid shear stiffness estimations using 2-D spatial excitations in magnetic resonance elastography. In: Proc 10th Annual Meeting ISMRM, 2002:39.
18. Pauly J, Nishimura D, Macovski A. A k-space analysis of small-tip-angle excitation. J Magn Reson Imaging 1989;81:43–56.
19. Kim DH, Adalsteinsson E, Spielman DM. Simple analytic variable density spiral design. Magn Reson Med 2003;50:214–219.
20. Hardy CJ, Cline HE. Broadband nuclear magnetic resonance pulses with two-dimensional spatial selectivity. J Appl Physiol 1989;66:1513–1516.
21. Sack I, McGowan CK, Samani A, Luginbuhl C, Oakden W, Plewes DB. Observation of nonlinear shear wave propagation using magnetic resonance elastography. Magn Reson Med 2004;52:842–850.